À Propos Stars Departing from Giant Branches

Alfred Gautschy

September 22, 2024

CBmA, 4410 Liestal, Switzerland

After stars evolved far enough along the first or the asymptotic giant branch they depart therefrom. Once the envelope mass becomes low enough, the stars' effective temperatures rise at roughly constant luminosity. To gain a better understanding of this canonical phenomenon, the stellar-physical processes that affect the turn-away from the giant branches are discussed.

Phenomenology

Stars that evolve along the Hayashi line to higher luminosities, either in H-shell or combined He-/H-burning mode, leave the so called giant branch at some point to evolve to higher effective temperatures without changing the luminosity. For stars arriving directly from their main-sequence phase, the giant branch is usually referred to as the First Giant Branch (FGB). Post core – He-burning stars ascend the giant branch again; then they trace out the so called Asymptotic Giant Branch (AGB). In the following, the notion of the Giant Branch (GB) refers generically to FGB *and* AGB.

The central question of this manuscript is: What causes stars that evolve along a GB to eventually depart from it and evolve to higher effective temperatures?

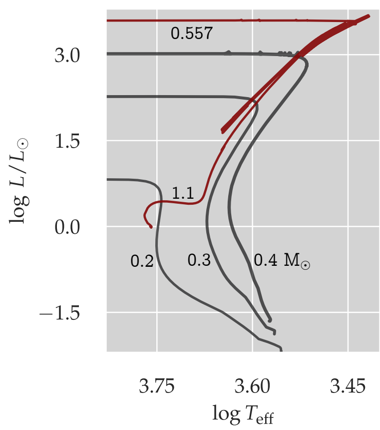

Figure 1: Evolutionary tracks of a set of low- and intermediate-mass stars that start from the $X = 0.7, Z = 0.02$ ZAMS.

FOR CANONICAL H-RICH STARS, the phenomenon of terminating the GB ascent is illustrated in Fig. 1. Most of the models are very-low mass (VLM) stars that do not ignite He core-burning. For comparison, the approach to and evolution along the Hayashi line of an initially 1.1 $M_\odot$ low-mass (LM) star, whose mass shrinks eventually to 0.557 $M_\odot$, is added to the figure in red. The ascent along the AGB ends around $2 \times 10^3\, L_\odot$ in double-shell nuclear-burning mode when the star's mass is down at about $0.67 M_\odot$ due to an computationally imposed mass-loss.

The evolutionary tracks of the VLM model stars show that all of them live through a phase of a rather steep luminosity rise, even before they are close to what looks like their respective Hayashi lines. Eventually, the VLM stars curve to higher temperatures to evolve away from the GB; the ensuing evolution proceeds at essentially constant luminosity. The maximum luminosity at which the stars depart from the FGB correlates with M_* (cf. Fig. 1). The behavior is comparable with the low- and intermediate-mass stars that generate their nuclear energy via double-shell burning as they ascend the

AGB. In absence of thermal shell instabilities, also these stars depart from the AGB to evolve quickly to high effective temperatures at roughly constant luminosity. The maximum luminosity they achieve on the AGB correlates with $M_*(t)$.

Figure 2 tracks the relative *envelope masses* of the H-rich V/LM model stars as a function of T_{eff}. Evolution changes from going cooler to getting hotter once the envelope masses fall below 10 to 20 % of the total mass.

At around the turn-away epochs from the GB (see Fig. 3) one finds that:

- The envelopes of the H-rich VLM/LM stars have structure radiative-zero at temperatures between the nuclear-burning shell and about 10^6K at the base of the envelope convection zones (ECZs).
- As the stars' masses grow, the envelope profiles on the $\log \rho - \log T$ plane get closer to the $P_{\text{g}} = P_{\text{rad}}$ line over ever more extended ranges in depth.
- In VLM models, up to about 0.5 M_* (inner core), the stellar matter is degenerate, the rest of the core is, in good approximation, an ideal gas.

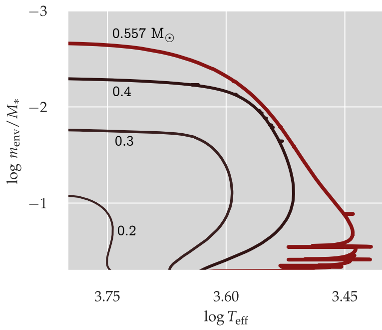

Figure 2: VLM- and LM-stars terminate evolution along the GB once their envelope masses get low enough.

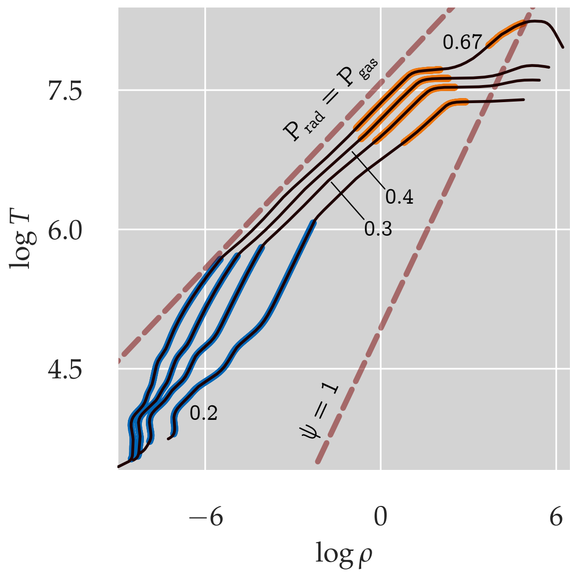

Figure 3: PopI VLM and LM structure profiles around the epochs of respective turn-aways from their GBs. Blue lines: ECZs. Orange regions: nuclear-burning shells. The 0.67 ($M_\odot$) locus belongs to the star that terminates its life with 0.557 $M_\odot$.

Single VLM stars that leave the FGB cannot be observed in nature, the Universe is not yet old enough to harbor them. Though, close binary stars might come to rescue: In case a primary component loses enough mass to its lower-mass companion in a case-B scenario, the donor's envelope mass might drop below the critical value to inflict departure from the GB. Further evolution might take such a stripped star into the instability strip where it pulsates not unlike an RR-Lyr variable, though with a deviating mass. A star of this new class of pulsators, baptized BEP variables, might have been identified in the massive photometric monitoring project OGLE (Smolec et al. 2013).

PURE ELECTRON-SCATTERING OPACITY POPI MODELS evolve on the HR plane much like their PopI brethren with naturalistic opacities. The tracks are merely stretched to lower effective temperatures because the overly simplified constant-opacity models do not adhere to the Hayashi limit inflicted by the H^- contribution to realistic-opacity models but they continue to cool as they grow brighter. Figure 4 contrasts the evolution on the HR plane of e^--scattering – opacity models to PopI full-opacity VLM ones. As can be seen, the terminal luminosity at the departure from the GB is roughly the same for e^--scattering – opacity and for full-opacity models.

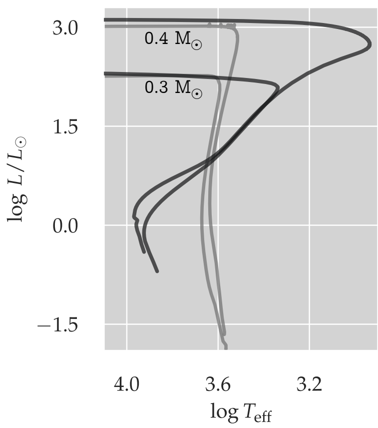

Figure 4: Evolutionary tracks of e^--scattering – opacity models (black). The gray tracks are those of corresponding-mass models shown in Fig. 1.

Most importantly: Also the e^- – scattering opacity models terminate their evolution to high luminosities once the envelope on top of the H-burning shell gets thin enough (in mass). Figure 5 highlights the relevant region along the effective-temperature axis when the e^--scattering – opacity models start to depart from the GB. Departure comes once $m_{\rm env}/M_* \approx 0.1$ (0.3 $M_\odot$ sequence) and 0.16 (0.4 $M_\odot$ sequence), respectively.

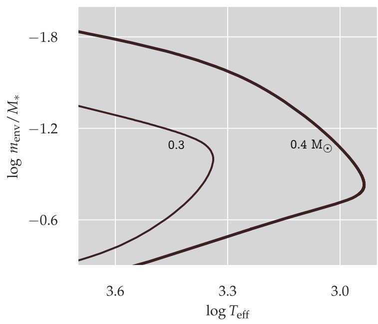

Figure 5: Relative envelope mass of e^--scattering – opacity models along their GBs.

The envelopes of the e^--scattering – opacity models all have essentially radiative-zero structure (cf. Fig. 6) because the constant opacity does not induce extended ECZs. The local reduction of $\nabla_{\rm ad}$ in the zones of partial ionization of He and H induces nonetheless narrow superficial convective zones.

- The envelopes of the H-rich e^--scattering opacity VLM stars have radiative-zero envelope structures that extend from the nuclear-burning shell to the very superficial layers.
- At the turn-aways from the GBs, about 0.5 M_* (the inner core) is degenerate. The stellar matter in the deep mantle between core and H-burning shell is, to a good approximation, an almost isothermal ideal gas.

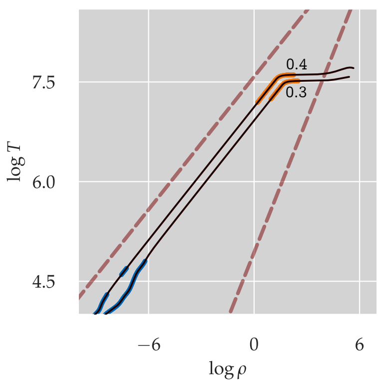

Figure 6: PopI VLM structure profiles of pure e^--scattering opacity models around the epochs of respective turn-aways from the GB.

EVOLUTIONARY TRACKS OF LOW-MASS HE-STARS behave topologically like their H-rich brethren: The collection of tracks in Fig. 7 belongs to low-mass helium stars with 0.6, 0.7, and 0.8 $M_\odot$. These stars start their evolution on the helium-star ZAMS (HeZAMS) with a homogeneous composition of Y = 0.98, Z = 0.02. During core and ensuing shell He-burning, He-stars get brighter with growing radii. At some stage during He shell-burning, also the helium stars evolve to higher $T_{\rm eff}$ without much further raising their luminosities. The 0.6 $M_\odot$ sequence does not approach the He-star giant region at all. The more massive stars turn away from the GBs with $m_{\rm env}/M_* \approx 0.19$ for 0.7 $M_\odot$ and $m_{\rm env}/M_* \approx 0.09$ for the 0.8 $M_\odot$ sequence, respectively (Fig. 8).

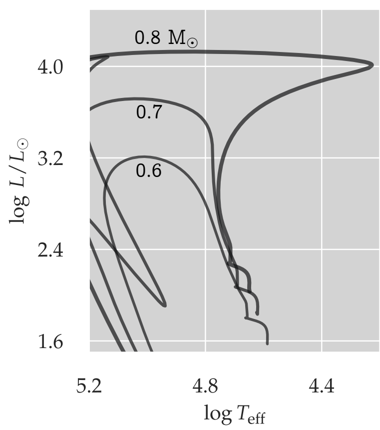

Figure 7: Selected evolutionary tracks off the HeZAMS ($Y = 0.98, Z = 0.02$).

During all these evolutionary phases, the He-stars are so hot that their envelopes are essentially purely radiative. The very superficial, shallow ECZ do not significantly deflect the envelope stratification from radiative-zero structures (Fig. 9). Once the He-stars turn away from their GBs, radiation pressure is important in the outer envelopes of all model sequences considered.

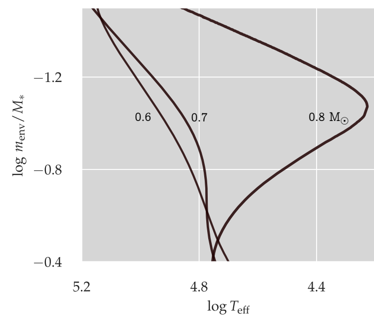

Figure 8: As for the H-rich stars, also He-stars tend to leave the 'giant branch' at sufficiently low envelope mass.

Hence, once again, the process that forces the loci of the stars on the HR plane away from the giants' habitat does not depend on extensive ECZs such as they are encountered in full-opacity H-rich stars along the FGB.

At the turn-aways from the He-stars' GB:

- The envelopes of low-mass He-stars have radiative-zero structure between the nuclear-burning shell and about 10^5 K.
- Envelope structures (on the $\log\rho - \log T$ plane) evolve toward the $P_{\rm g} = P_{\rm rad}$ line. Below a few times 10^5K, the envelopes of the more massive stars can even become radiation-pressure dominated.
- The regions of $\lesssim 0.5\,M_*$ (inner core) are degenerate. The lower the mass of the He-stars, the less massive is the ideal-gas mantle on top of the inner core, which has a temperature gradient inflicted by $\nu-$losses.

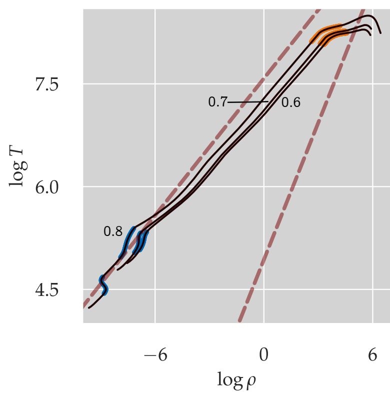

Figure 9: He-stars' structure profiles around the epochs of their respective turn-aways from the GB. Colored and dashed lines are the same as in Fig. 3. The numbers label the stellar masses in solar units. Radiation pressure is substantial in these hot low-mass He stars.

ALL THINGS CONSIDERED regarding the termination of FGB and AGB evolution. For the *existence* of a turn-away from the respective GB:

- The mode of energy transport (convection/radiation diffusion) is not important.
- Chemical composition of the stars is not important.
- Opacity details are not important.
- Evolutionary tracks of any flavor of model stars turn away from the GBs once $m_{\rm env}/M_*$ drops to $\mathcal{O}(0.1)$.

An explanation ansatz

To understand the T_{eff}-evolution as a star's core mass grows, focus on approximations to the *energy-transport equation*; its formal integration in depth (measured in $\log P$) from the surface to the H-burning shell and subsequent differentiation wrt. $\log m_{\text{core}}$ yields:

$$\frac{\mathrm{d}\log T_{\text{eff}}}{\mathrm{d}\log m_{\text{core}}} = \frac{\mathrm{d}\log T_{\text{sh}}}{\mathrm{d}\log m_{\text{core}}} + \langle\nabla\rangle \left[\frac{\mathrm{d}\log P_{\text{phot}}}{\mathrm{d}\log m_{\text{core}}} - \frac{\mathrm{d}\log P_{\text{sh}}}{\mathrm{d}\log m_{\text{core}}}\right] . \quad (1)$$

The quantity $\langle\nabla\rangle$ is the average value of the temperature gradient across the integrated envelope. The subscript 'phot' refers to the photosphere, physical quantities measured at maximum nuclear burning, are tagged by 'sh'. The maximum of nuclear burning lies near the bottom of the nuclear active shell so that the region closer to the star's center is accordingly referred to as the stellar core, the rest belongs to the envelope.

Equation 1 is the result of elementary mathematical manipulations only. All the physics is embedded in ∇. The particular physical details are not relevant in the following because $\nabla(m)$ – independently of the prevailing energy transport process – does not greatly vary throughout the envelope; most importantly, it is bounded from above: In the simplest case of a convectively unstable (adiabatic) ideal, mono-atomic-gas: $\nabla(m) = \nabla_{\text{ad}} = \text{const.} = 0.4$. In ionization zones, $0.1 \lesssim \nabla_{\text{ad}} < 0.4$.

N.B.: for $P_{\text{rad}} \gg P_{\text{g}}$: $\nabla_{\text{ad}} \to 1/4$

Close to the outer boundary of superficial ECZs, where convection goes nonadiabatic due to energy losses, eventually $\nabla \to \nabla_{\text{rad}}$ and usually exceeds unity. Nevertheless, the mostly narrow super-adiabatic convection regions with their ∇ spikes do not substantially affect $\langle\nabla\rangle$. On the other hand, in regions where energy is transported by photon diffusion: $0 < \nabla(m) = \nabla_{\text{rad}}(m) < \nabla_{\text{ad}}$. Therefore, for further estimates we can quite safely assume the fore-factor to the square bracket on the rhs of eq. 1 to be

$$0 \lesssim \langle\nabla\rangle \lesssim 1\,.$$

Adopting the concept of a *shell-source homology* (ssh) as introduced by Refsdal & Weigert (1970) and extended by Kippenhahn (1981) who included the effect of radiation pressure, the following relations can be derived: Assuming CNO burning and electron-scattering opacity at the nuclear-burning shell, the case of *negligible radiation pressure* yields:

$$\frac{\mathrm{d}\log T_{\text{sh}}}{\mathrm{d}\log m_{\text{core}}} = 1 - \frac{\mathrm{d}\log R_{\text{sh}}}{\mathrm{d}\log m_{\text{core}}}\,,$$

$$\frac{\mathrm{d}\log P_{\text{sh}}}{\mathrm{d}\log m_{\text{core}}} = -2 + \frac{4}{3}\frac{\mathrm{d}\log R_{\text{sh}}}{\mathrm{d}\log m_{\text{core}}}\,;$$

on the other hand, if *radiation pressure dominates*, the above derivatives become:

$$\frac{\mathrm{d}\log T_{\text{sh}}}{\mathrm{d}\log m_{\text{core}}} = \frac{1}{7} - \frac{5}{21}\frac{\mathrm{d}\log R_{\text{sh}}}{\mathrm{d}\log m_{\text{core}}}\,,$$

$$\frac{\mathrm{d}\log P_{\mathrm{sh}}}{\mathrm{d}\log m_{\mathrm{core}}} = \frac{4}{7} - \frac{20}{21}\frac{\mathrm{d}\log R_{\mathrm{sh}}}{\mathrm{d}\log m_{\mathrm{core}}}\,.$$

The derivative $\mathrm{d}\log R_{\mathrm{sh}}/\mathrm{d}\log m_{\mathrm{core}}$ is not a priori determined in the ssh modeling.

Despite the surface pressure (P_{phot}) being much lower than the shell pressure (P_{sh}) it is its variation as a function of core mass that can render it potentially important. The fact that the formulation of the mechanical surface boundary-condition is essentially at the discretion of the modeler does not ease the quantification of its effect.

Integrate the hydrostatic equation through the atmosphere:

$$\int_{P=0}^{P_{\mathrm{phot}}} \mathrm{d}P = \int_{\tau=0}^{2/3} \frac{g}{\varkappa}\mathrm{d}\tau\,,$$

with $g = Gm/r^2$. If $\varkappa$ does not vary wildly, $P_{\mathrm{phot}} \propto R_*^{-2}$ can be expected. Hence:

$$\frac{\mathrm{d}\log P_{\mathrm{phot}}}{\mathrm{d}\log m_{\mathrm{core}}} \approx -2\,\frac{\mathrm{d}\log R_*}{\mathrm{d}\log m_{\mathrm{core}}}\,.$$

The following plot grids, one grid for each set of model sequences, illustrate the variation of the physical quantities that are relevant to compute the three rhs – terms of eq. 1: R_{sh}, T_{sh}, P_{sh}, P_{phot} as a function of m_{core}. The slopes that enter eq. 1 were estimated from the plot frames in the neighborhood of the turn-away epochs with ruler and pocket calculator[1]. In Figs. 10 - 12, the turn-away epochs can be derived from the upper-left plot panels of the respective plots.

[1] The old-fashioned approach proved very efficient because the data lines are numerically noisy: The shell location was equated with the cell of maximum nuclear energy generation but the actual physical maximum usually lies somewhere between two cells.Therefore, the numerical noise is an effect of discretization.

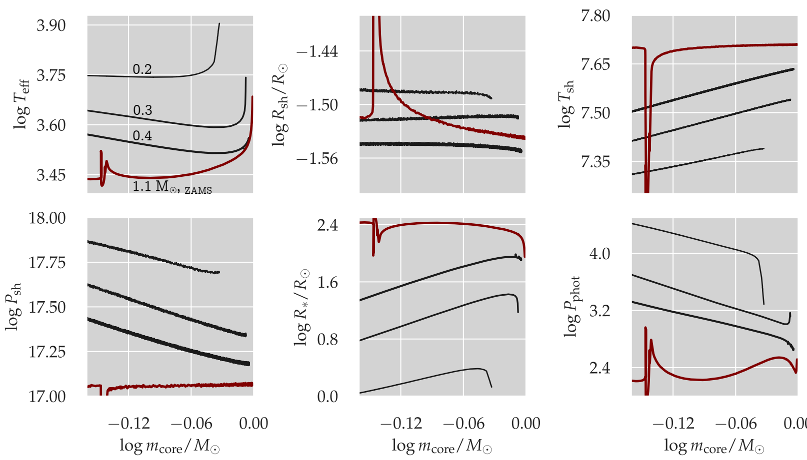

Figure 10: Pertinent H-shell and photospheric quantities of H-rich stars as a function of core-mass (mass interior to the H-burning shell). The slopes of the various loci enter the analytical analysis. The red lines come from the model with $M_{\mathrm{ZAMS}} = 1.1 M_\odot$ around its departure from the AGB.

H-RICH STARS COMPUTED WITH CANONICAL $\varkappa$-TABLES: All three VLM models behave similarly (Fig.10). The curves are typically parallel shifted relative to each other. In all models, P_{sh} decreases as m_{sh} (i.e. m_{core}) grows, in contrast T_{sh} increases. On the other hand, R_{sh} hardly varies over the whole relevant m_{core} range. The LM star (of $M_{\mathrm{ZAMS}} = 1.1 M_\odot$, leaving the AGB with $\approx 0.67 M_\odot$;

red loci in Fig.10) behaves differently though. This might be caused by the additional active He-burning shell in the deeper core and/or the star's evolving out of a thermal pulse at the top of the AGB.

Environment	$\frac{\mathrm{d}\log T_{\mathrm{sh}}}{\mathrm{d}\log m_{\mathrm{sh}}}$	$\frac{\mathrm{d}\log P_{\mathrm{phot}}}{\mathrm{d}\log m_{\mathrm{sh}}}$	$\frac{\mathrm{d}\log P_{\mathrm{sh}}}{\mathrm{d}\log m_{\mathrm{sh}}}$	$\frac{\mathrm{d}\log R_{\mathrm{sh}}}{\mathrm{d}\log m_{\mathrm{sh}}}$
H-rich VLM	0.7 - 0.9	-3 – -5	-1.5 – -1.9	0
ssh, $P \approx P_{\mathrm{g}}$	1		-2	
ssh, $P \approx P_{\mathrm{rad}}$	1/7		4/7	

In the table above, $\mathrm{d}\log R_{\mathrm{sh}}/\mathrm{d}\log m_{\mathrm{sh}} = 0$ entered the quantification of the ssh relations. The VLM-models' evolution seems to be compatible with the H-shell changing homologously in a gas-pressure dominated environment.

Environment	$\frac{\mathrm{d}\log T_{\mathrm{sh}}}{\mathrm{d}\log m_{\mathrm{sh}}}$	$\frac{\mathrm{d}\log P_{\mathrm{phot}}}{\mathrm{d}\log m_{\mathrm{sh}}}$	$\frac{\mathrm{d}\log P_{\mathrm{sh}}}{\mathrm{d}\log m_{\mathrm{sh}}}$	$\frac{\mathrm{d}\log R_{\mathrm{sh}}}{\mathrm{d}\log m_{\mathrm{sh}}}$
1.1 $M_{\odot,\mathrm{ZAMS}}$	0.1	≈ 0	0.2	-0.6
ssh, $P \approx P_{\mathrm{g}}$	1.6		-2.8	
ssh, $P \approx P_{\mathrm{rad}}$	2/7		1.1	

For the thermally pulsing $M_{\mathrm{ZAMS}} = 1.1 M_{\odot}$ sequence, the radius of the H-shell shrinks with about $\mathrm{d}\log R_{\mathrm{sh}}/\mathrm{d}\log m_{\mathrm{sh}} \approx -0.6$ around the turn-away phase. The situation is more complicated than for the H-rich VLM models because AGB stars have in addition to the H-burning shell also an intermittently dominating He-burning shell on the top of an inner CO-core.

H-RICH STARS WITH $\varkappa$(e^--SCATTERING) OPACITY ONLY:

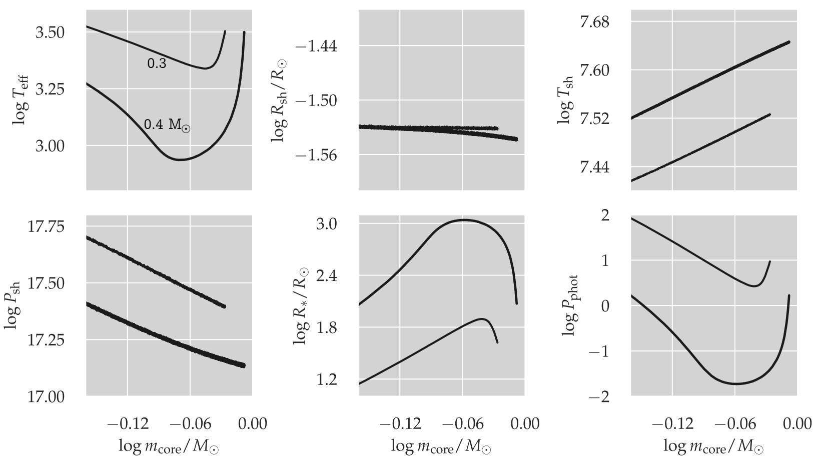

Figure 11: Same as Fig. 10 but for $\varkappa$(e^--scattering) – only VLM model stars.

Environment	$\frac{\mathrm{d}\log T_{\mathrm{sh}}}{\mathrm{d}\log m_{\mathrm{sh}}}$	$\frac{\mathrm{d}\log P_{\mathrm{phot}}}{\mathrm{d}\log m_{\mathrm{sh}}}$	$\frac{\mathrm{d}\log P_{\mathrm{sh}}}{\mathrm{d}\log m_{\mathrm{sh}}}$	$\frac{\mathrm{d}\log R_{\mathrm{sh}}}{\mathrm{d}\log m_{\mathrm{sh}}}$
H-rich stars w/ $\varkappa(\mathrm{e}^-)$	0.7 – 0.9	-23 – -13	-2.4 – -2.1	≈ 0
ssh, $P \approx P_{\mathrm{g}}$	1		-2	
ssh, $P \approx P_{\mathrm{rad}}$	1/7		4/7	

Also the H-rich stars with simplified opacity law (e^--scattering only) obey essentially the ssh prescription in the gas-pressure dominated regime (compatible with Fig. 6). The stars' radii grow strongly. The very simple opacity reveals that indeed $\mathrm{d}\log P_{\mathrm{phot}}/\mathrm{d}\log R_* = -2$ obtains.

HELIUM STARS:

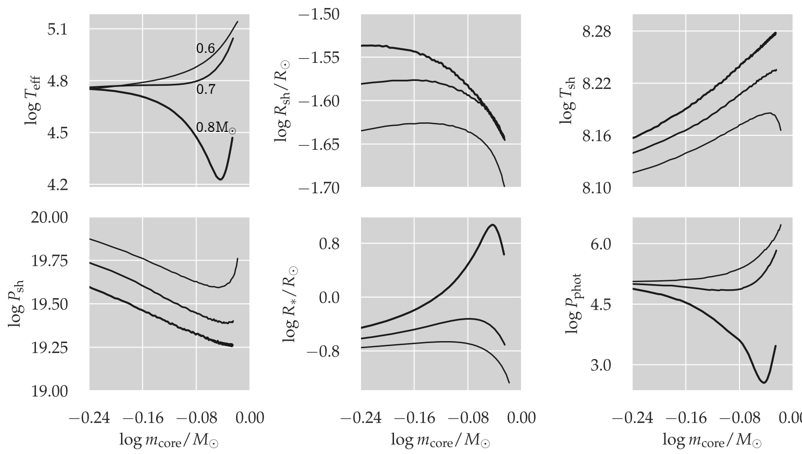

Figure 12: Same as Fig. 10 but for low-mass He-stars.

Environment	$\frac{\mathrm{d}\log T_{\mathrm{sh}}}{\mathrm{d}\log m_{\mathrm{sh}}}$	$\frac{\mathrm{d}\log P_{\mathrm{phot}}}{\mathrm{d}\log m_{\mathrm{sh}}}$	$\frac{\mathrm{d}\log P_{\mathrm{sh}}}{\mathrm{d}\log m_{\mathrm{sh}}}$	$\frac{\mathrm{d}\log R_{\mathrm{sh}}}{\mathrm{d}\log m_{\mathrm{sh}}}$
He stars	0.4 – 0.7	-10 – 1	-2 – -1	$\approx$ -1 – 0.2
ssh, $P \approx P_{\mathrm{g}}$	2 – 0.8		-3.3 – -1.7	
ssh, $P \approx P_{\mathrm{rad}}$	0.4 – 0.1		1.5 – 0.4	

In the ssh rows, the first numbers refer to $\mathrm{d}\log R_{\mathrm{sh}}/\mathrm{d}\log m_{\mathrm{sh}} \approx -1$; the second entries go with the slope of 0.2, respectively. The variation of P_{phot} remains anti-correlated with that of R_* but the characteristic exponent in $P_{\mathrm{phot}} \propto R_*^{-\alpha}$ varies along an evolutionary sequence and in particular between the different He-star sequences.

In the He-star models, the effect of P_{rad} is most expressed in the outer envelope. The magnitude of $\mathrm{d}\log T_{\mathrm{sh}}/\mathrm{d}\log m_{\mathrm{sh}}$ appears to be in the range preferred by radiation-pressure dominated ssh. On the other hand, the variation of P_{sh} is compatible with a gas-pressure dominated ssh. All in all, radiation pressure appears not to be important for the physical behavior of the nuclear-burning shell.

PUTTING IT ALL TOGETHER: In all three modeling sequences presented above, the evolution of T_{sh} and P_{sh} as a function of m_{core} is reasonably compatible with the predictions of ssh for a gas-pressure dominated shell region. Radiation pressure affects only the late AGB evolution of the $1.1 M_{\odot,\mathrm{ZAMS}}$ and the He-star models. The predictions of ssh relied on *computed* R_{sh} behavior; its evolution remains to be understood independently of the ssh ansatz.

The direction of the T_{eff} evolution as a function of m_{core}, as prescribed by eq. 1, is determined by two terms. The first one on the rhs is always positive; i.e. the steady increase of the shell temperature tries to increase the star's surface temperature. This tendency is counteracted by the difference of the pressure slopes at the surface and at the shell, respectively. The second rhs term is moderated by the fore-factor $\langle \nabla \rangle$, which is inconspicuous as it is always positive and less than unity. This latter point means that the mode of energy transport in a star's envelope is irrelevant for the T_{eff} evolution along and at the end of the GB. The computations of H-rich (V)LM models and pure $\varkappa(\mathrm{e}^-$-scattering) as well as He-star models support this. Hence, it is the difference of the two pressure gradients (P_{phot} and P_{sh}) in the square bracket of eq. 1 that decides over the direction in which T_{eff} evolves. The freedom of the modeler to formulate outer mechanical boundary conditions when modeling stars makes it difficult to put forth reliable numbers while the stars evolve along the GBs. The general trend of $P_{\mathrm{phot}} \propto R_*^{-2}$, points at least to a helpful direction. The tables presented indicate that the $\mathrm{d}\log P_{\mathrm{phot}} / \mathrm{d}\log m_{\mathrm{core}}$ term dominates usually over $\mathrm{d}\log P_{\mathrm{sh}} / \mathrm{d}\log m_{\mathrm{core}}$, in particular at small core masses. Hence, $\mathrm{d}\log P_{\mathrm{phot}} / \mathrm{d}\log m_{\mathrm{core}} < 0$ enforces the star models to evolve to lower effective temperatures with growing core mass.

In almost all cases, $\mathrm{d}\log P_{\mathrm{sh}} / \mathrm{d}\log m_{\mathrm{core}} < 0$ because the hydrostatic pressure at the nuclear burning shell gets smaller with the ever reduced envelope mass (with the shell radius remaining stationary). The decreasing shell pressure contributes therefore to rising effective temperatures. In the end it is the competition between $\mathrm{d}\log P_{\mathrm{phot}} / \mathrm{d}\log m_{\mathrm{core}}$ and $\mathrm{d}\log P_{\mathrm{sh}} / \mathrm{d}\log m_{\mathrm{core}}$ that determines the eventual direction of evolution. Because P_{phot} mostly anti-correlates with the star's radius, it is the orientation of the GB locus relative to lines of constant radius that decides when/if a star starts to turn away from the GB.

Once a star evolves off its GB and its radius starts to shrink, the $\mathrm{d}\log P_{\mathrm{phot}} / \mathrm{d}\log m_{\mathrm{core}}$ term might (if the $\varkappa$-contribution to the photospheric pressure is negligible) even turn into an accelerator of further evolution to higher effective temperatures. This effect is seen in the VLM $\varkappa(\mathrm{e}^-)$-only and the He-star model sequences.

REMAINING ISSUES: The answers found so far are at best partial. Mostly, the problems were just moved to another level:

- Why is $\mathrm{d}\log R_{\mathrm{sh}}/\mathrm{d}\log m_{\mathrm{core}} \approx 0$ so frequently and why is the rule broken in the case of He-stars – a class of stars that otherwise behaves along the giant branch essentially like the H-rich brethren?
- Enforcing $P_{\mathrm{phot}} = $ const. in stellar evolution computations should affect the turn-away epoch and behavior from the GB. A vanishing $\mathrm{d}\log P_{\mathrm{phot}}/\mathrm{d}\log m_{\mathrm{core}}$ should induce a trend for respective stars to evolve to higher T_{eff} earlier during their shell-burning evolution. (N.B. Such an `MESA` experiment is possible.)
- Why do the shell sources evolve homologously at all? What is the star's benefit of doing so? The same question applies also to homology relations that prevail to some degree in the complete (chemically homogeneous) stars.
- Even though the GB evolution of the model stars seem to mostly conform to ssh, the case is not always overwhelmingly clear. Most of all, it is striking how *how discrepant* figures like Fig. 10 – 12 are and hence also how discrepant the derived slopes would be if ssh does not prevail.

CONJECTURE: The evolution of the lowest-mass, i.e. the hottest horizontal-branch stars toward the subdwarf region on the HR diagram is likely also driven by the critical thinning of the envelope overlying the He-burning stellar core. It would be worthwhile to add this case to the set of models discussed here to eventually fit them all into a common framework.

References

Kippenhahn, R. 1981, A&A, 102, 293

Refsdal, S. & Weigert, A. 1970, A&A, 6, 426

Smolec, R., Pietrzyński, G., Graczyk, D., et al. 2013, MNRAS, 428, 3034

Version 1.1 - 2024.IX